

3D Beamforming for Improving the Security of UAV-Enabled Mobile Relaying System

Quan-sheng YUAN, Yong-jiang HU, Chang-long WANG, Xiao-lin MA

Dept. of Unmanned Aerial Vehicle Engineering, Shijiazhuang Campus of Army Engineering University, Shijiazhuang, China

{yuanquan140, huyongjiangoec, wangchanglongoec,maxiaolinoec}@126.com

Submitted August 16, 2018 / Accepted December 20, 2018

Abstract. *In this paper, we consider an unmanned aerial vehicle (UAV)-enabled mobile relaying system consists of a ground control station (GCS), a high-mobility UAV for relaying, a destination, and an eavesdropper. To improve the security of the three-dimension (3D) mobile relaying system with delayed channel state information (CSI), we propose a destination-specific (DS) 3D beamforming scheme and an eavesdropper-null (EN) 3D beamforming scheme, in both the horizontal angle and the vertical angle of antenna pattern are adapted instantaneously. In particular, we study the secrecy rate maximization problem via trajectory planning. However, this problem with mobility constraint and location constraint is a non-convex optimization problem. To solve it, we propose a successive trajectory planning algorithm by optimizing the incremental in each time-slot. Simulation results verify that the 3D beamforming schemes can greatly improve the security of UAV-enabled mobile relaying system and the proposed trajectory planning algorithm is also proven become effective.*

Keywords

Unmanned aerial vehicle (UAV), physical layer security, 3D beamforming, secrecy rate, trajectory planning

1. Introduction

In recent years, unmanned aerial vehicles (UAVs) attract much attention in civic area as well as military application, for UAVs are cost-effective and operate easily now [1–3]. In some scenarios, such as search-and-rescue in disaster, emergency inspection, and high risk tactical communication, it is effective to deploy UAV as a relay [4], [5]. Due to involved data of these missions are sensitive, the relay UAV is an interesting target for cyber attack. On the other hand, the channels in UAV communication system, UAV-UAV links or UAV-ground control station (GCS) links, are wireless communication channel, which is vulnerable to eavesdroppers. It is necessary to develop an efficient secure communication infrastructure to protect signals between UAVs and equipment on the ground, and

physical layer security is a good option [6], [7].

Pioneered by Wyner [8], physical layer security exploits characters of wireless channel to achieve secure communication without secret key encryption. Beamforming, as a signal processing approach, has become an important aspect in research of physical layer security. Prior researches on beamforming for improving security are mainly two-dimension (2D) beamforming [9–12], which is beamforming in horizontal plane. However, due to the three-dimension (3D) nature of wireless channel between UAVs and GCS/destination, with 3D directional antennas in UAVs, 3D beamforming [13–15] can fully exploit the secrecy degrees of freedom in signal transmission.

Motivated by this, we propose two secrecy schemes based on 3D beamforming, destination-specific to maximize the receive power at the destination, and eavesdropper-null to null out receive power at the eavesdropper. In both two schemes above, the horizontal angle and the vertical angle can be adapted instantaneously, thus increase the signal intensity in desired direction. When channel state information (CSI) of UAVs communication system is imperfect due to delay, the secrecy rate of proposed schemes is analyzed. Furthermore, trajectory planning is an important and challenging task in UAV system [16], [17]. Different from optimization objectives in prior works, we propose a successive trajectory planning algorithm to make secrecy rate maximization via optimizing the trajectory incremental in each time-slot, subject to mobility constraint and location constraint.

2. System Model

As shown in Fig. 1, we consider a 3D UAV-enabled mobile relaying communication model, which consists of a source node S , a destination node D , a relay node R and an eavesdropper node E . In practical, S is a GCS equipped with N_s antennas, D may be a wireless sensor equipped with an antenna, and R is a UAV equipped with N_r antennas. In this paper, there is no direct link between S and D/E due to distance or blockage such as terrain or buildings. This assumption is reasonable for military or rescue in earthquake.

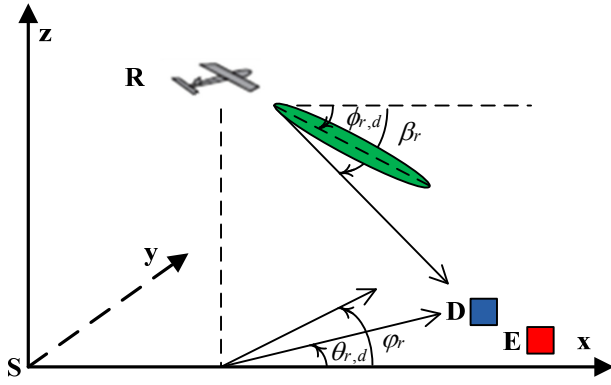


Fig. 1. 3D beamforming in UAV-enabled mobile relaying system.

To introduce the 3D beamforming at R , the 3GPP 3D directional antenna model is incorporated, in which the antenna gain between R and D is expressed in dBi as [18]

$$G_{r,d} = - \left(\min \left[12 \left(\frac{\theta_{r,d} - \varphi_r}{\theta_{3dB}} \right)^2, SLL_{az} \right] + \min \left[12 \left(\frac{\phi_{r,d} - \beta_r}{\phi_{3dB}} \right)^2, SLL_{el} \right] \right) + G_m. \quad (1)$$

As depicted in Fig. 1, in (1), $\theta_{r,d}$ is the angle of the line connecting R and D away from x -axis in the horizontal direction, φ_r is the orientation angle of the array boresight at R away from x -axis, θ_{3dB} is the half-power beamwidth in the horizontal plane, SLL_{az} is the side lobe level in the horizontal plane of antenna pattern. Furthermore, $\phi_{r,d}$, β_r , ϕ_{3dB} and SLL_{el} are corresponding values in the vertical direction, while G_m is the peak antenna gain. According to commonly used Kathrein 742215 antenna, we set $\theta_{3dB} = 65^\circ$, $\phi_{3dB} = 6^\circ$, $SLL_{az} = 30$ dB, $SLL_{el} = 18$ dB, $G_m = 18$ dBi. It is worth noting that $\theta_{r,d}$ and $\phi_{r,d}$ in this paper are varying due to the mobility of the UAV.

Likewise, the antenna gain between R and E can be expressed in dBi as [18]

$$G_{r,e} = - \left(\min \left[12 \left(\frac{\theta_{r,e} - \varphi_r}{\theta_{3dB}} \right)^2, SLL_{az} \right] + \min \left[12 \left(\frac{\phi_{r,e} - \beta_r}{\phi_{3dB}} \right)^2, SLL_{el} \right] \right) + G_m. \quad (2)$$

We consider a Cartesian coordinate system model depicted in Fig. 1, in which S located at $(0, 0, 0)$, D located at $(x_d, y_d, 0)$, E located at $(x_e, y_e, 0)$. Assuming the hovering height of UAV is fixed at H , thus, R has a time-varying coordinate, which can be expressed as $(x(t), y(t), H)$, $0 \leq t \leq T$, where $x(t)$ and $y(t)$ denoting the instantaneous x - and y -coordinates of R . T is the time for hovering and is discretized into N equal spaced time-slots, i.e., $T = NT_s$, where T_s is small sufficiently so the location of UAV can be considered as approximately constant in each time-slot. Thus, the trajectory of UAV, i.e., $\{x(t), y(t)\}$, can be approximated by sequences $\{x(n), y(n)\}_{n=1}^N$.

There are two phases in the data transmission process from S to D . The GCS S sends source information to the relay UAV R in the first phase. In the second phase, the relay UAV R sends confidential message x_r to D . To highlight the effect of the relay, we focus on downlink transmission from R to D , i.e., the second phase. Assuming narrow-band flat-fading channel model, the received complex baseband discrete-time signal in time-slot n is

$$y_d[n] = \sqrt{\alpha_{r,d}} \mathbf{h}_{r,d}^H[n] \mathbf{w}[n] x_r[n] + z_d[n]. \quad (3)$$

In (3), $\mathbf{h}_{r,d}[n] \in \mathbb{C}^{N_r \times 1}$ is the channel vector between R and D and has i.i.d $\theta \mathcal{CN}(0,1)$ elements, $(\cdot)^H$ denotes complex conjugate transpose, $\mathbf{w}[n] \in \mathbb{C}^{N_r \times 1}$ is the associated beamforming vector, $z_d[n]$ is the additive Gaussian white noise with zero mean and variance σ_d^2 at D , $\alpha_{r,d}$ is given as

$$\alpha_{r,d} = PL_{r,d} G_{r,d} \quad (4)$$

where $PL_{r,d}$ denotes the pathloss between R and D .

Likewise, we can get the received complex baseband discrete-time signal at the eavesdropper as

$$y_e[n] = \sqrt{\alpha_{r,e}} \mathbf{h}_{r,e}^H[n] \mathbf{w}[n] x_r[n] + z_e[n] \quad (5)$$

where $\mathbf{h}_{r,e}[n] \in \mathbb{C}^{N_r \times 1}$ is the channel vector between R and E and has i.i.d $\mathcal{CN}(0,1)$ elements, $z_e[n]$ is the additive Gaussian white noise with zero mean and variance σ_e^2 at E , $\alpha_{r,e}$ is given as

$$\alpha_{r,e} = PL_{r,e} G_{r,e} \quad (6)$$

where $PL_{r,e}$ denotes the pathloss between R and E .

3. Secrecy Rate with Delayed CSI

3.1 Beamforming Scheme

Beamforming strategy can be designed in two folds, beamforming vector design and beamforming angle design. We consider two beamforming vector design methods firstly, i.e., destination-specific and eavesdropper-null.

1) Beamforming Vector Design

Destination-specific (DS): In this strategy, the UAV attempts to maximize the received power at the destination by pointing the beamforming direction to the destination, in which the beamforming vector is expressed as

$$\mathbf{w}^{DS}[n] = \frac{\mathbf{h}_{r,d}[n]}{\|\mathbf{h}_{r,d}[n]\|}. \quad (7)$$

Eavesdropper-null (EN): In this strategy, by nulling out signals at the eavesdropper, the secrecy rate can be improved, then, $\mathbf{h}_{r,e}^H[n] \mathbf{w}^{EN}[n] = 0$. Denoting P as the transmit power at the UAV, the optimal eavesdropper-null beamforming vector with the power constraint P is given by [19]

$$\boldsymbol{\omega}^{\text{EN}}[n] = \frac{\sqrt{P}}{\|(\mathbf{I}_{N_r} - \mathbf{P}_{r,e}[n])\mathbf{h}_{r,d}[n]\|} (\mathbf{I}_{N_r} - \mathbf{P}_{r,e}[n])\mathbf{h}_{r,d}[n] \quad (8)$$

where $\mathbf{P}_{r,e}[n] = \mathbf{h}_{r,e}[n](\mathbf{h}_{r,e}^H[n]\mathbf{h}_{r,e}[n])^{-1}\mathbf{h}_{r,e}^H[n]$.

2) Beamforming Angle Design

In this scheme, we adjust the horizontal angle and vertical angle to the location of destination immediately. In UAVs communication system, location information is available through positioning system. Furthermore, the immediate angle adjustment electronically is feasible to feed identical signals having appropriate phase shift with multiple antenna elements [13]. Mathematically, this scheme can be expressed as

$$\begin{aligned} \varphi_r &= \theta_{r,d}, \\ \beta_r &= \phi_{r,d}. \end{aligned} \quad (9)$$

3.2 Secrecy Rate

There have been much works about study on secrecy rate, for the case of one eavesdropper, the secrecy rate at destination in time-slot n is [20]

$$R_s[n] = R_d[n] - R_e[n] \quad (10)$$

where R_d is the achievable rate of the link between R and D , R_e is the achievable rate of the link between R and E , furthermore, R_d and R_e in time-slot n can be expressed as

$$R_d[n] = \frac{1}{2} \log_2 (1 + \gamma_d[n]), \quad (11)$$

$$R_e[n] = \frac{1}{2} \log_2 (1 + \gamma_e[n]) \quad (12)$$

where γ_d and γ_e represent the signal-to-noise ratios of the links from R to D and E , the scalar factor $1/2$ is due to the fact that two phases are needed in the data transmission from S to D . Then, γ_d and γ_e in time-slot n can be expressed as

$$\gamma_d[n] = \frac{\alpha_{r,d} \|\mathbf{h}_{r,d}^H[n]\boldsymbol{\omega}[n]\|^2 P}{\sigma_d^2}, \quad (13)$$

$$\gamma_e[n] = \frac{\alpha_{r,e} \|\mathbf{h}_{r,e}^H[n]\boldsymbol{\omega}[n]\|^2 P}{\sigma_e^2} \quad (14)$$

where σ_d^2 and σ_e^2 mean the variances of terminal noise at the destination and the eavesdropper, $\boldsymbol{\omega}[n] = \boldsymbol{\omega}^{\text{DS}}[n]$ if destination-specific beamforming strategy is adopted, and $\boldsymbol{\omega}[n] = \boldsymbol{\omega}^{\text{EN}}[n]$ if eavesdropper-null beamforming strategy is adopted.

With the delay in CSI acquisition, we consider Gauss-Markov block-fading autoregressive model, then $\mathbf{h}_{r,d}[n]$ in (13) and $\mathbf{h}_{r,e}[n]$ in (14) are expressed as [21]:

$$\mathbf{h}_{r,d}[n] = \rho_{r,d} \mathbf{h}_{r,d}[n - D_d] + \sqrt{1 - \rho_{r,d}^2} \mathbf{e}_{r,d}[n], \quad (15)$$

$$\mathbf{h}_{r,e}[n] = \rho_{r,e} \mathbf{h}_{r,e}[n - D_e] + \sqrt{1 - \rho_{r,e}^2} \mathbf{e}_{r,e}[n] \quad (16)$$

where D_d and D_e denote the CSI delays from R to D and E , $\rho_{r,d}^2$ and $\rho_{r,e}^2$ are the CSI estimation error variances of links from R to D and E , $\mathbf{e}_{r,d}[n]$ and $\mathbf{e}_{r,e}[n]$ denote the error version of channel vectors in time-slot n and have i.i.d $\mathcal{CN}(0,1)$ elements. It is worth noting that $\mathbf{e}_{r,d}[n]$ and $\mathbf{e}_{r,e}[n]$ are uncorrelated with $\mathbf{h}_{r,d}[n - D_d]$ or $\mathbf{h}_{r,e}[n - D_e]$. Furthermore, based on Clarker's autocorrelation model [22], [23], $\rho_{r,d}$ and $\rho_{r,e}$ are determined as

$$\rho_{r,d} = J_0(2\pi D_d f_d T_s), \quad (17)$$

$$\rho_{r,e} = J_0(2\pi D_e f_d T_s) \quad (18)$$

where $J_0(\cdot)$ means 0-th order Bessel function of the first kind, f_d denotes the Doppler spread which is expressed as

$$f_d = \frac{v f_c}{c} \quad (19)$$

where v denotes the velocity of UAV, f_c denotes carrier frequency, c means the speed of light.

Then, we can get the expression of secrecy rate as

$$R_s[n] = \frac{1}{2} \log_2 \left(\frac{1 + \frac{P}{\sigma_d^2} \alpha_{r,d} \|\mathbf{h}_{r,d}^H[n]\boldsymbol{\omega}[n]\|^2}{1 + \frac{P}{\sigma_e^2} \alpha_{r,e} \|\mathbf{h}_{r,e}^H[n]\boldsymbol{\omega}[n]\|^2} \right) \quad (20)$$

where P is the transmit power at the UAV, $\mathbf{h}_{r,d}[n]$ and $\mathbf{h}_{r,e}[n]$ can be obtained from (15)-(19).

4. Trajectory Planning

Notice that the UAV has mobility constraint as

$$(x[n] - x[n-1])^2 + (y[n] - y[n-1])^2 \leq (vT_s)^2, \quad n = 1, \dots, N. \quad (21)$$

Besides, the UAV has location constraint, i.e., the initial location and the final location. For simplicity, we suppose the initial location of the UAV is at the hovering height over the GCS, and the final location of UAV is $\{x_d, y(N)\}$. Thus, the trajectory optimization problem is to maximize the secrecy rate in time-slot n with mobility constraint and location constraint, which can be formulated as follows.

$$\begin{aligned} \text{(P1):} \quad & \max_{\{x[n], y[n]\}} R_s[n] \\ \text{s.t.} \quad & (x[n] - x[n-1])^2 + (y[n] - y[n-1])^2 \leq (vT_s)^2, \quad (22) \\ & x[0] = 0, \quad y[0] = 0, \quad x[N] = x_d, \\ & n = 1, \dots, N. \end{aligned}$$

We assume $x[n] = x[n-1] + \varepsilon[n]$, $y[n] = y[n-1] + \delta[n]$, i.e., $\{\varepsilon[n], \delta[n]\}$ denote the trajectory incremental in time-slot n . This assumption is helpful to solve (P1). Besides,

$\varepsilon[n]$ is always positive in reality. Then (P1) can be written as

$$(P2): \quad \max_{\{x[n], y[n]\}} R_s[n]$$

$$\text{s.t.} \quad \varepsilon^2[n] + \delta^2[n] \leq (vT_s)^2, n = 1, \dots, N, \quad (23)$$

$$x[0] = 0, y[0] = 0, x[N] = x_d,$$

$$\varepsilon[n] > 0.$$

Due to the mobility constraint, the maximal secrecy rate at any location is subjected to the location of the previous time-slot, thus (P2) can be translated to the problem of secrecy rate difference value maximization of time-slot n and time-slot $n-1$ as follows.

$$(P3): \quad \max_{\{x[n], y[n]\}} R_s[n] - R_s[n-1]$$

$$\text{s.t.} \quad \varepsilon^2[n] + \delta^2[n] \leq (vT_s)^2, n = 1, \dots, N, \quad (24)$$

$$x[0] = 0, y[0] = 0, x[N] = x_d,$$

$$\varepsilon[n] > 0.$$

(P3) is a non-convex problem. For simplicity, we assume the UAV is hovering at constant speed v , then the hovering distances in each time-slot are same as vT_s . As $\varepsilon[n] > 0$, the location of next time-slot is at a semicircle whose center is the location of current time-slot. In the following, we propose a successive trajectory optimization algorithm, in which the secrecy rate difference value of time-slot n and time-slot $n-1$ is maximized by choosing appropriate heading angle λ in each time-slot.

In Algorithm 1 and simulation in the next section, we define pathloss $PL_{r,d}$ in (4) and $PL_{r,e}$ in (6) as $PL_{r,d(e)} = -(128.1 + 37.6 \log(L_{r,d(e)}))$ in dB [18], in which $L_{r,d}$ denotes the distance between the UAV and the destination in km, $L_{r,e}$ denotes the distance between the UAV and the eavesdropper in km. $L_{r,d(e)}$ in time-slot n can be expressed as

$$L_{r,d(e)}[n] = \sqrt{h^2 + (x_{d(e)} - x[n])^2 + (y_{d(e)} - y[n])^2}. \quad (25)$$

5. Numerical Results and Discussion

In this section, the performance of proposed schemes are evaluated through Monte Carlo simulation. 3D directional antennas are assumed at the unmanned aerial vehicle (UAV). Based on Fig. 1, we consider two typical UAV models with search-and-find mission, i.e., building searching and low-altitude searching. In building searching model, the hovering altitude is 100 m, the maximum flying distance is 2000 m, and the maximum velocity is 40 km/h; whereas in low-altitude searching model, the hovering altitude is 400 m, the maximum flying distance is 5000 m, and the maximum velocity is 80 km/h. In practical, the ground control station (GCS) is always a vehicle below 3 m, thus it is reasonable to neglect its height. The transmit power at the relay UAV is set as 10 dBm, while the noise power at destination and eavesdropper is assumed as -169 dBm equally. In each simulation, all channel vectors

Algorithm 1 Successive trajectory planning algorithm

```

Initialize
 $x[0] = 0, y[0] = 0, \varepsilon[0, 0] = 0, \delta[0, 0] = 0, n = 1,$ 
Repeat
 $x[n] = x[n-1] + \varepsilon[n-1, \text{index}(n-1)],$ 
 $y[n] = y[n-1] + \delta[n-1, \text{index}(n-1)],$ 
If  $x[n] < x_d$ 
Calculate  $R_s[n-1],$ 
for  $k = \lambda \in [1, \dots, 179]$ 
 $\varepsilon[n, k] = \sin \lambda \cdot (vT_s), \delta[n] = \cos \lambda \cdot (vT_s),$ 
 $x[n, k] = x[n-1] + \varepsilon[n, k], y[n, k] = y[n-1] + \delta[n, k],$ 
calculate  $R_s[n, k],$ 
get  $R_s[n, k] - R_s[n-1],$ 
 $\{\max_r(n), \text{index}(n)\} = \max(R_s[n, k] - R_s[n-1]),$ 
end for
 $n = n + 1,$ 
else
break
end if
Output  $\{x[n], y[n]\}.$ 
    
```

are random and the results are obtained by averaging the instantaneous secrecy rate over 1000 fading realizations.

5.1 Effect of 3D Beamforming for Secrecy Rate

In this subsection, we compare the secrecy rates of proposed 3D beamforming schemes, destination-specific (DS) and eavesdropper-null (EN). There are four types of benchmark schemes, no-vector-design 3D beamforming (NV), no-beamforming (NB), maximal ratio transmission (MRT) with 2D beamforming (MRT-2D), zero forcing (ZF) with 2D beamforming (ZF-2D) [24]. In NV scheme, the UAV adjusts the beamforming angle in each time-slot, whereas the beamforming vector is not designed. The NB scheme is defined as the scheme that the UAV relays message without beamforming. The trajectory of UAV is predetermined and fixed. As shown in Fig. 2, in NB scheme, secrecy rates always fall down below 0. When 3D beamforming is adopted, NV can get positive secrecy rate. We also observe that MRT-2D and ZF-2D show similar performance compared with DS and EN, however, the secrecy rates of MRT-2D and ZF-2D fall down below 0 sometimes as the tilt cannot change with the flying of the UAV. As expected, DS and EN get higher secrecy rate than NV. The proposed schemes perform well even when the eavesdropper is between GCS and destination as we can see from Fig. 2(b).

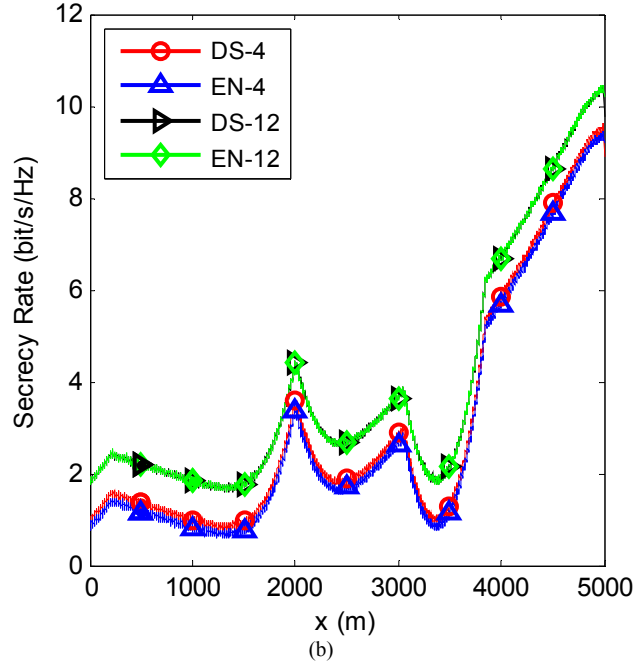
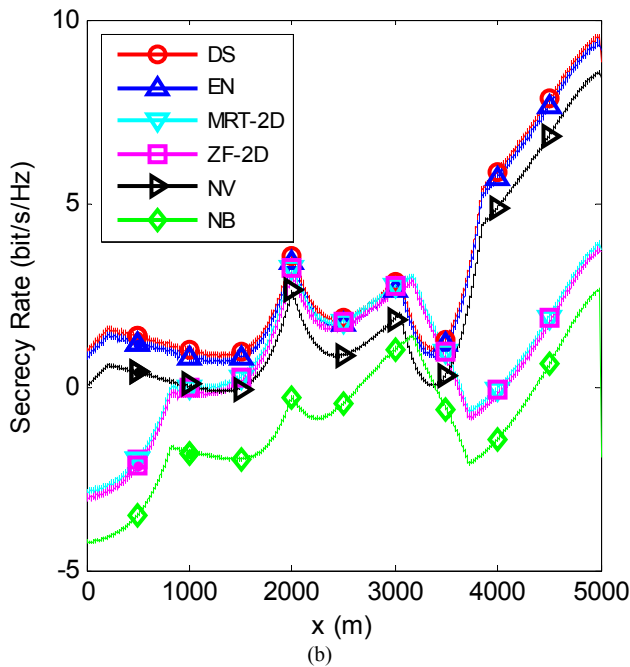
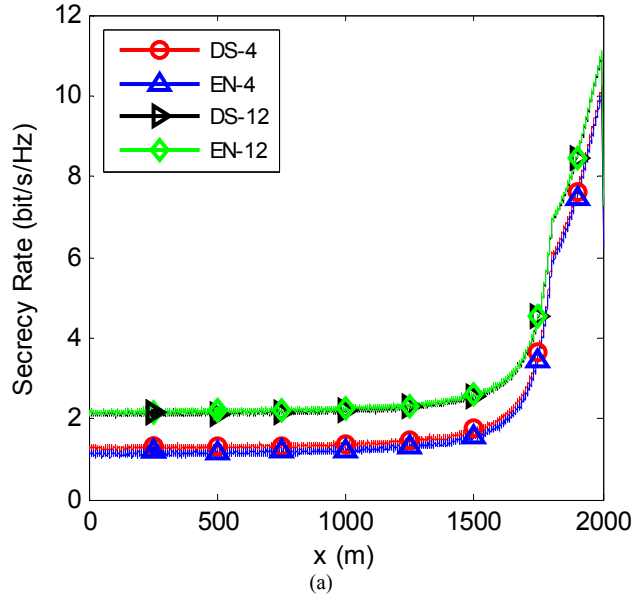
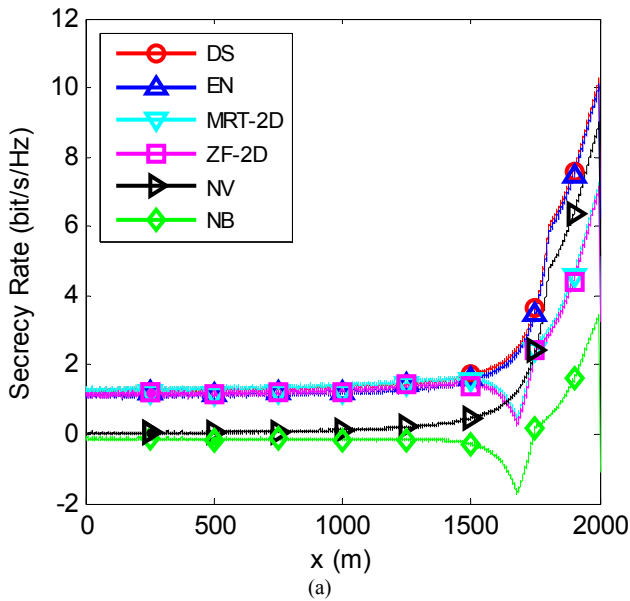


Fig. 2. Secrecy rate versus x-coordinate of relay among different beamforming scheme. In (a), the destination location is fixed at (2000,0,0), the eavesdropper location is fixed at (2000,-200,0). In (b), the destination location is fixed at (5000,0,0), the eavesdropper location is fixed at (2000,500,0). The UAV flying unidirectional from S to D. The number of relay antenna is $N_r = 4$.

Fig. 3. Secrecy rate versus x-coordinate of relay among different beamforming scheme of different antenna number. In (a), the destination location is fixed at (2000,0,0), the eavesdropper location is fixed at (2000,-200,0). In (b), the destination location is fixed at (5000,0,0), the eavesdropper location is fixed at (2000,500,0). The UAV flying unidirectional from S to D. The number of relay antenna is $N_r = 4$ in (a) and is $N_r = 12$ in (b).

5.2 Effect of Antenna Number for Secrecy Rate

As observed in Fig. 3, the secrecy rates increase along with the accretion of antenna number. We can see from Fig. 2 and Fig. 3 that the secrecy performances of DS and EN are comparative.

5.3 Effect of Delay for Secrecy Rate

Figure 4 shows secrecy rates of different 3D beamforming schemes for different delays at the destination or the eavesdropper. There are three schemes in Fig. 4: 1) DS-D1E7 or DS-D7E1, when DS scheme is adopted, the channel state information (CSI) delay from R to D, i.e., D_a ,

is set as 1 time-slot or 7 time-slots, the CSI delay from R to E , i.e., D_e , is set as 7 time-slots or 1 time-slot; 2) EN-D1E7 or EN-D7E1, when EN scheme is adopted, D_d is set as 1 time-slot or 7 time-slots, D_e is set as 7 time-slots or 1 time-slot; 3) NB-D0E0, NB scheme is adopted with perfect CSI. For DS-D7E1 and EN-D7E1, i.e., the CSI of relay-destination due to delay is worse than relay-eavesdropper, EN is the preferred scheme in two scenarios. It is because the signal of relay to eavesdropper is completely null out in EN. It can be easily concluded that EN is optimal scheme when the CSI of relay-eavesdropper is known at the relay UAV. It can be seen that with perfect CSI, the performance of NB scheme is still worse than DS or EN.

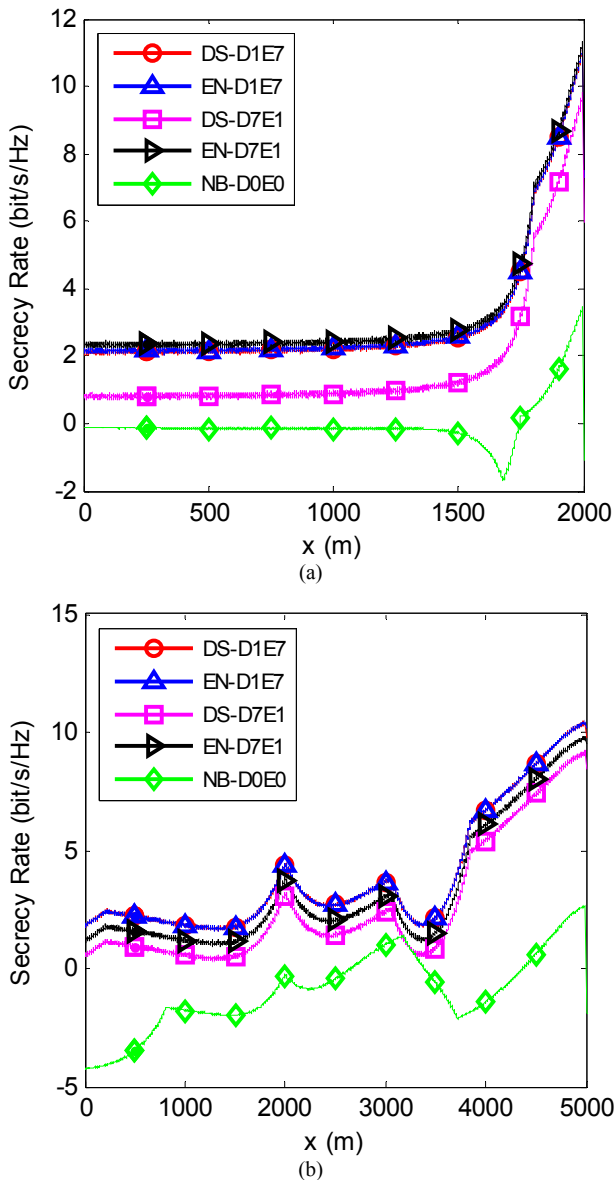


Fig. 4. Secrety rate versus x-coordinate of relay among different beamforming scheme for different delay. In (a), the destination location is fixed at (2000,0,0), the eavesdropper location is fixed at (2000,-200,0). In (b), the destination location is fixed at (5000,0,0), the eavesdropper location is fixed at (2000,500,0). The UAV flying unidirectional from S to D. The number of relay antenna is $N_r = 12$.

5.4 Effect of Trajectory for Secrecy Rate

To illustrate the effects of trajectory planning on secrecy rate, Figure 5 shows three trajectories: 1) DS-1 or EN-1, the UAV flies unidirectional from GCS to destination; 2) DS-2 or EN-2, the UAV flies slantways; 3) DS-T or EN-T, the UAV flies under trajectory planning. In Fig. 5(a), the eavesdropper is closer to the destination, then the secrecy rates are always nearly 2 bits/s/Hz when the UAV flying from 0 to 1500 m away from the GCS. On the other hand, the secrecy performances of trajectory planning and unidirectional from GCS to destination are almost the same due to the heading angle of trajectory planning is nearly 90° . In Fig. 5(b), it is demonstrated that trajectory planning can enhance the secrecy rate effectively.

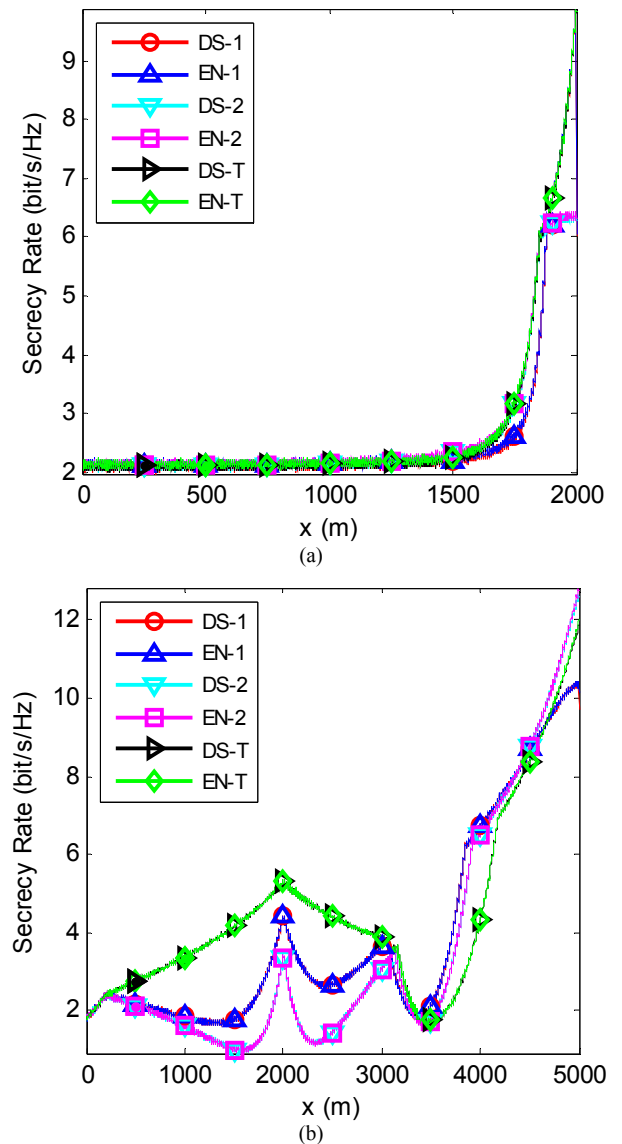


Fig. 5. Secrety rate versus x-coordinate of relay among different beamforming scheme of different trajectory. In (a), the destination location is fixed at (2000,0,0), the eavesdropper location is fixed at (2000,-200,0). In (b), the destination location is fixed at (5000,0,0), the eavesdropper location is fixed at (2000,500,0). The number of relay antenna is $N_r = 12$.

6. Conclusions

In this paper, we proposed two 3D beamforming schemes, DS and EN, to improve the security of UAV-enabled relaying system with delayed CSI. Furthermore, a successive trajectory algorithm is proposed to maximize the secrecy rate with the mobility constraint and the location constraint, via optimizing the incremental trajectory in each time-slot. The secrecy performance of different beamforming schemes and different system parameters are compared through simulation respectively. Also, numerical results showed that the trajectory planning algorithm is effective. Research on 3D beamforming of multiple-UAV relaying system and multiple-destination UAV-enabled relaying system are interesting issues for future work.

References

- [1] HAYAT, S., YANMAZ, E., MUZAFFAR, R. Survey on unmanned aerial vehicle networks for civil applications: a communications viewpoint. *IEEE Communication Surveys & Tutorials*, 2016, vol. 18, no. 4, p. 2624–2661. DOI: 10.1109/COMST.2016.2560343
- [2] ZENG, Y., ZHANG, R., LIM, T. J. Wireless communications with unmanned aerial vehicles: Opportunities and challenges. *IEEE Communication Magazine*, 2016, vol. 54, no. 5, p. 36–42. DOI: 10.1109/MCOM.2016.7470933
- [3] HASSAN, H., KHAN, M. N., GILANI, S. O., et al. H.264 encoder parameter optimization for encoded wireless multimedia transmissions. *IEEE Access*, 2018, vol. 6, p. 22046–22053. DOI: 10.1109/ACCESS.2018.2824835
- [4] CHAMSEDDINE, A., AKHRIF, O., CHARLAND-ARCAND, G., et al. Communication relay for multiground units with unmanned aerial vehicle using only signal strength and angle of arrival. *IEEE Transactions on Control Systems Technology*, 2017, vol. 25, no. 1, p. 286–293. DOI: 10.1109/TCST.2016.2552461
- [5] ZHAN, P., YU, K., LEE SWINDLEHURST, A. Wireless relay communications with unmanned aerial vehicles: performance and optimization. *IEEE Transactions on Aerospace and Electronic Systems*, 2011, vol. 47, no. 3, p. 2068–2085. DOI: 10.1109/TAES.2011.5937283
- [6] ZHANG, S., FAN, L., PENG, M., et al. Near-optimal modulo-and-forward scheme for the untrusted relay channel. *IEEE Transactions on Information Theory*, 2016, vol. 62, no. 5, p. 2545–2556. DOI: 10.1109/TIT.2016.2530080
- [7] WANG, Q., CHEN, Z., MEI, W., et al. Improving physical layer security using UAV-enabled mobile relaying. *IEEE Wireless Communication Letters*, 2017, vol. 6, no. 3, p. 310–313. DOI: 10.1109/LWC.2017.2680449
- [8] WYNER, A. D. The wire-tap channel. *Bell System Technical Journal*, 1975, vol. 54, no. 8, p. 1355–1387. DOI: 10.1002/j.1538-7305.1975.tb02040.x
- [9] OUYANG, N., JIANG, X., BAI, E., et al. Destination assisted jamming and beamforming for improving the security of AF relay systems. *IEEE Access*, 2017, vol. 5, p. 4125–4131. DOI: 10.1109/ACCESS.2017.2682838
- [10] LIU, L., ZHANG, R., CHUA, K. Secrecy wireless information and power transfer with MISO beamforming. *IEEE Transactions on Signal Processing*, 2014, vol. 62, no. 7, p. 1850–1863. DOI: 10.1109/TSP.2014.2303422
- [11] WING KWAN NG, D., LO, E. S., SCHOBBER, R. Robust beamforming for secure communication in systems with wireless information and power transfer. *IEEE Transactions on Wireless Communications*, 2014, vol. 13, no. 8, p. 4599–4615. DOI: 10.1109/TWC.2014.2314654
- [12] KHAN, M. N., RIZVI, U. H. Antenna beam-forming for a 60 GHz transceiver system. *Arabian Journal for Science and Engineering*, 2013, vol. 38, p. 2451–2464. DOI: 10.1007/s13369-013-0555-8
- [13] HALBAUER, H., SAUR, S., KOPPENBORG, J., et al. 3D beamforming: performance improvement for cellular networks. *Bell Labs Technical Journal*, 2013, vol. 18, no. 2, p. 37–56. DOI: 10.1002/bltj.21604
- [14] SEIFI, N., ZHANG, J., HEATH, R. W., et al. Coordinated 3D beamforming for interference management in cellular networks. *IEEE Transactions on Wireless Communications*, 2014, vol. 13, no. 10, p. 5396–5410. DOI: 10.1109/TWC.2014.2349981
- [15] NIU, J., LI, G. Y., LI, Y., et al. Joint 3D beamforming and resource allocation for small cell wireless backhaul in HetNets. *IEEE Communication Letters*, 2017, vol. 21, no. 10, p. 2286–2289. DOI: 10.1109/LCOMM.2017.2723008
- [16] ZENG, Y., ZHANG, R., LIM, T. J. Throughput maximization for UAV-enabled mobile relaying systems. *IEEE Transactions on Communications*, 2016, vol. 64, no. 12, p. 4983–4996. DOI: 10.1109/TCOMM.2016.2611512
- [17] ZENG, Y., XU, X., ZHANG, R., Y. Trajectory design for completion time minimization in UAV-enabled multicasting. *IEEE Transactions on Wireless Communications*, 2018, vol. 17, no. 4, p. 2233–2246. DOI: 10.1109/TWC.2018.2790401
- [18] 3rd Generation Partnership Project. *Further Advancements for E-UTRA Physical Layer Aspects (3GPP, TR 36.814 V9.2.0)*. 105 pages. [Online] Cited 2017-03. Available at: <http://www.tech-invite.com/3m36/tinv-3gpp-36-814.html#toc>
- [19] FRIEDLANDER, B., PORAT, B. Performance analysis of a null-steering algorithm based on direction-of-arrival estimation. *IEEE Transactions on Signal Processing*, 1989, vol. 37, no. 4, p. 461–466. DOI: 10.1109/29.17526
- [20] DONG, L., HAN, Z., PETROPULU, A. P., et al. Improving wireless physical layer security via cooperating relays. *IEEE Transactions on Signal Processing*, 2010, vol. 58, no. 3, p. 1875–1888. DOI: 10.1109/TSP.2009.2038412
- [21] MA, Y., ZHANG, D., LEITH, A., et al. Error performance of transmit beamforming with delayed and limited feedback. *IEEE Transactions on Wireless Communications*, 2009, vol. 8, no. 3, p. 1164–1170. DOI: 10.1109/TWC.2008.080570
- [22] CLARKE, R. H. A statistical theory of mobile-radio reception. *Bell System Technical Journal*, 1968, vol. 47, no. 6, p. 957–1000. DOI: 10.1002/j.1538-7305.1968.tb00069.x
- [23] TAN, C. C., BEAULIEU, N. C. On first-order Markov modeling for the Rayleigh fading channel. *IEEE Transactions on Communications*, 2000, vol. 48, no. 12, p. 2032–2040. DOI: 10.1109/26.891214
- [24] HUANG, Y., WANG, J., ZHONG, C. et al. Secure transmission in cooperative relaying networks with multiple antennas. *IEEE Transactions on Wireless Communications*, 2016, vol. 15, no. 10, p. 6483–6856. DOI: 10.1109/TWC.2016.2591940

About the Authors ...

QUAN-SHENG YUAN received the B.S. degree in Communication Engineering from the University of Electronic Science and Technology of China, Chengdu, China, in 2013 and the M.S. degree in Unmanned Aerial Vehicle Engineering from the Ordnance Engineering College, Shijiazhuang, China, in 2016. He is currently pursuing the

Ph.D. degree in Unmanned Aerial Vehicle Engineering at Shijiazhuang Campus of Army Engineering University, Shijiazhuang, China. His main research interests include UAV-assisted communication and physical layer security.

YONG-JIANG HU received the B.S. degree in fire command and control from the Ordnance Engineering College, the M.S. degree in Electronic and Communication Engineering from Shanghai Jiaotong University, and Ph.D. degree in Navigation Guidance and Control from the Ordnance Engineering College. He is currently an Associate Professor with the Department of Unmanned Aerial Vehicle Engineering, Shijiazhuang Campus of Army Engineering University, Shijiazhuang, China. His main research interests include UAV-assisted communication and physical layer security.

CHANG-LONG WANG (corresponding author) received the B.S. degree in Radar Engineering from the Electronic

Engineering College, Hebei, China, in 1987, the M.S. degree in Signal and Information Processing from Harbin Institute of Technology, Harbin, China, in 1992, and Ph.D. degree in Signal Processing from Xi'an Jiaotong University, Xi'an, China, in 2006. He is currently a Professor with the Dept. of Unmanned Aerial Vehicle Engineering, Shijiazhuang Campus of Army Engineering University, Shijiazhuang, China. His main research interests include UAV-assisted communication and signal processing.

XIAO-LIN MA received B.S. degree in Electronics from Hebei University of Technology, and the M.S. degree in Microwave from the Communication University of China. She is currently an Associate Professor with the Dept. of Unmanned Aerial Vehicle Engineering, Campus of Army Engineering University, Shijiazhuang, China. Her main research interests include UAV-assisted communication and anti-jamming.